

Recoverin Improves Rod-Mediated Vision by Enhancing Signal Transmission in the Mouse Retina

Report

Alapakkam P. Sampath,^{1,7} Katherine J. Strissel,³
Rajesh Elias,⁴ Vadim Y. Arshavsky,³
James F. McGinnis,⁴ Jeannie Chen,⁵
Satoru Kawamura,⁶ Fred Rieke,¹
and James B. Hurley^{2,*}

¹Department of Physiology and Biophysics

²Department of Biochemistry

University of Washington

Seattle, Washington 98195

³Howe Laboratory of Ophthalmology

Harvard Medical School

The Massachusetts Eye and Ear Infirmary

Boston, Massachusetts 02114

⁴Departments of Cell Biology and Ophthalmology

University of Oklahoma Health Science Center

Oklahoma City, Oklahoma 73104

⁵Department of Ophthalmology

Zilkha Neurogenetic Institute

Keck School of Medicine

University of Southern California

Los Angeles, California 90089

⁶Department of Biology

Graduate School of Science

Osaka University

Toyonaka, Osaka 560-0043

Japan

Summary

Vision in dim light requires that photons absorbed by rod photoreceptors evoke signals that reliably propagate through the retina. We investigated how a perturbation in rod physiology affects propagation of those signals in the retina and ultimately visual sensitivity. Recoverin is a protein in rods that prolongs phototransduction and enhances visual sensitivity. It is not present in neurons postsynaptic to rods, yet we found that light-evoked responses of rod bipolar and ganglion cells were shortened when measured in recoverin-deficient retinas. Unexpectedly, the effect of recoverin on postsynaptic signals could not be explained by its effect on phototransduction. Instead, it is an effect of recoverin downstream of phototransduction in rods that prolongs signal transmission and enhances visual sensitivity. An important implication of our findings is that the recovery phase of the rod photoresponse does not contribute significantly to visual sensitivity near absolute threshold.

Introduction

The high sensitivity of scotopic, or rod-mediated, vision requires that rods detect single photons (Baylor et al.,

1979b; Baylor et al., 1984; reviewed by Field et al., 2005) and that the resulting signals are reliably propagated across the retina to produce a noticeable change in the retina's output (Barlow et al., 1971). In this study, we investigated the influence of the Ca²⁺ binding protein recoverin (Rv) on signal transmission in the retina and on visual sensitivity.

Photoactivation of rhodopsin in rods initiates a G protein-mediated signaling cascade that hyperpolarizes the rod and ultimately slows glutamate release at its synaptic terminal. The shutoff of rod phototransduction is important for scotopic vision. In particular, the shutoff of rhodopsin is essential, because a photoresponse will persist as long as rhodopsin is active. The shutoff of rhodopsin's catalytic activity requires phosphorylation of its C terminus (Chen et al., 1995; Chen et al., 1999). Rv inhibits rhodopsin phosphorylation in vitro (Kawamura, 1993), and physiological evidence suggests that it regulates the quenching of phototransduction in rods. Dialysis of Rv into a rod outer segment (OS) prolongs light responses (Gray-Keller et al., 1993; Erickson et al., 1998), and a genetic deficiency of Rv shortens the rod light response (Makino et al., 2004).

Using Rv-deficient mice, we found that Rv enhances scotopic vision, and we investigated the retinal mechanisms underlying this effect. We found that Rv prolongs the responses of rods, rod bipolar cells, and ganglion cells. Unexpectedly, however, the prolongation of rod responses could not explain the prolongation of downstream responses and could not account for the ability of Rv to enhance visual sensitivity. Our findings show instead that Rv enhances vision in dim light by enhancing signal transfer from rods to rod bipolar cells.

Results

Recoverin Increases the Sensitivity of Rod-Mediated Vision

We estimated thresholds for scotopic vision of *Rv*^{+/+} and *Rv*^{-/-} mice using a water maze (Figure 1A). The apparatus and strategy for evaluating visual threshold have been described (Hayes and Balkema, 1993; see Experimental Procedures). Each trial was initiated by releasing a mouse at the center of the maze. The back walls of five chambers of the maze were white, and the sixth wall, associated with a ramp and platform, was black. Mice were trained to find the black wall and were tested at various light intensities.

We compared the performance of nine *Rv*^{+/+} mice and nine *Rv*^{-/-} siblings derived from crosses of four sets of *Rv*^{+/-} parents. Figure 1B plots the time taken to find the platform (relative to the time in complete darkness) versus the intensity of light reflected from the white walls. Visual threshold, the light intensity at which the time to find the platform was 50% of that in darkness, was ~4-fold higher in *Rv*^{-/-} mice.

The conversion of light intensity in the water maze to photoisomerizations per rod (Rh*) depends on pupil size (Lyubarsky and Pugh, 1996). Pupil size was nearly

*Correspondence: jbh@u.washington.edu

⁷Present address: Department of Physiology and Biophysics, Zilkha Neurogenetic Institute, Keck School of Medicine, University of Southern California, Los Angeles, California 90089.

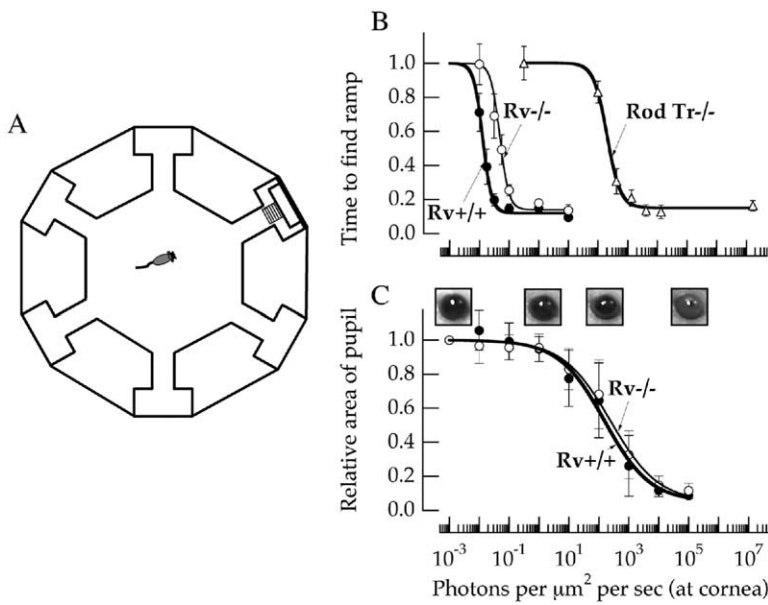


Figure 1. Recoverin Improves the Sensitivity of Rod-Mediated Vision

(A) A schematic of the water maze used to measure scotopic threshold (Hayes and Balkema, 1993). The white background illumination was spatially uniform. It was generated by reflecting the output from a halogen source off a diffuser over the maze. The black wall reflects 3%–4% of the light reflected by the white wall. Mice were placed in the center of the maze, and the time taken to reach the platform was measured.

(B) Collected results from nine *Rv*^{+/+} and nine *Rv*^{-/-} mice (all siblings from *Rv*^{+/-} crosses). The time required to find the ramp relative to the time required in complete darkness (~20 s) is plotted versus the intensity of light reflected from the white walls of the maze. Visual threshold was defined as the light intensity at which the time to find the platform was 50% of that in darkness. At visual threshold, the light intensity at the cornea, expressed in equivalent 501 nm photons (see Experimental Procedures), was 0.012 ± 0.002 photons/ $\mu\text{m}^2/\text{s}$ in *Rv*^{+/+} mice and 0.047 ± 0.009 photons/ $\mu\text{m}^2/\text{s}$ in *Rv*^{-/-} mice (mean \pm SEM; $n = 9$ each). A similar analysis of five rod transducin-deficient mice (*Tr*^{-/-})

is also included in order to show the lower limit of cone-mediated vision and therefore the range over which rods must be functional. Visual threshold in *Tr*^{-/-} rods was 200 photons/ $\mu\text{m}^2/\text{s}$.

(C) Pupil areas were measured in unanesthetized mice ($n = 7$ for each strain) in the water maze under the same illumination used for behavior. Maximal area was 3.93 ± 1.14 mm² for *Rv*^{+/+} and 3.95 ± 1.16 mm² for *Rv*^{-/-} (mean \pm SD).

constant across the range of illumination where escape times for *Rv*^{+/+} and *Rv*^{-/-} mice depended on light intensity (Figure 1C; see Experimental Procedures). Assuming a rod collecting area at the cornea of $0.2 \mu\text{m}^2$ (Lyubarsky and Pugh, 1996; see Experimental Procedures), visual threshold was 0.0024 ± 0.0005 Rh*/s for *Rv*^{+/+} mice and 0.009 ± 0.002 Rh*/s for *Rv*^{-/-} mice (mean \pm SEM; $n = 9$ each). Since the integration time of rod signals is approximately 0.2 s (Walraven et al., 1990), the threshold for this behavior occurs when 1 out of ~2000 (*Rv*^{+/+}) or 1 out of ~500 (*Rv*^{-/-}) rods absorbs a photon per integration time. Under these circumstances, behavior is guided by single photon absorptions in a small fraction of the rods in the retina.

To confirm that this behavior was mediated only by rods, we also analyzed rod transducin^{-/-} mice (Calvert et al., 2000). Since these mice use only cones for seeing, the light levels at which they begin to use visual cues define the upper end of the range over which vision is mediated exclusively by rods. rod transducin^{-/-} mice exhibited visually guided behavior only at light levels above 100 photons/ $\mu\text{m}^2/\text{s}$ (Figure 1B). In total, the range of background light intensity over which rods contribute to visual behavior is about 4 orders of magnitude. The action of Rv provides an ~4-fold enhancement at the lower end of this range.

Recoverin Influences Signal Transmission through the Retina

To determine how Rv influences behavioral threshold, we compared flash responses of rods, rod bipolar cells, and retinal ganglion cells in *Rv*^{+/+} and *Rv*^{-/-} retinas. Because photon absorptions are rare at behavioral thresh-

old, we measured responses to the weakest flashes that were practical (~1 Rh* for rods, <1 Rh* per rod for other cell types).

Rods

We used suction electrodes to record flash responses from *Rv*^{+/+} (Figure 2A) and *Rv*^{-/-} rods (Figure 2D). The relationship between peak amplitude and flash strength (Figure 2G) showed that *Rv*^{+/+} and *Rv*^{-/-} rods had similar flash sensitivities (Table 1; see also Makino et al., 2004). However, *Rv*^{-/-} responses returned to baseline more quickly than *Rv*^{+/+} responses at all flash strengths, consistent with previous reports (Makino et al., 2004). Dim flash responses of the two types of rods had a similar time to peak, but the integration time (response integral divided by peak amplitude) was shorter in *Rv*^{-/-} rods (Table 1). The time course of rod photocurrents in these experiments was similar to the time course in the intact eye (see the Supplemental Data available with this article online).

Rod Bipolar Cells

To determine how altered rod responses influenced downstream processing in the retina, we recorded flash responses from rod bipolar cells, the first neurons in a specialized mammalian pathway that transmits signals near visual threshold (Dacheux and Raviola, 1986; Sterling et al., 1988). Rv appears to be present only in rods, cones, and a subset of OFF bipolar cells (Milam et al., 1993; McGinnis et al., 1997), and hence Rv's influence on signals in the rod bipolar pathway is restricted to the rods themselves.

Figures 2B and 2E show flash families for rod bipolar cells from *Rv*^{+/+} and *Rv*^{-/-} retinas. The relationship between peak response amplitude and flash strength was similar for *Rv*^{+/+} and *Rv*^{-/-} rod bipolar cells (Figure 2H).

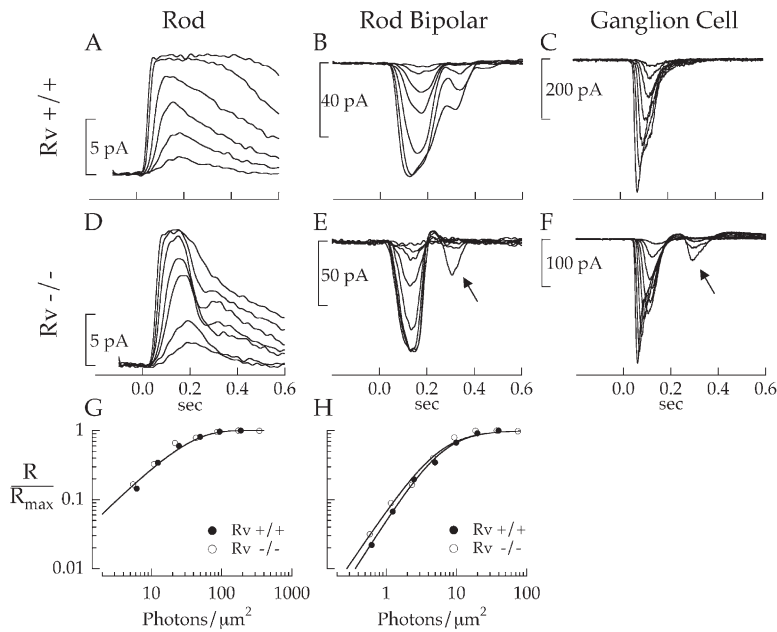


Figure 2. Rv Prolongs Light Responses of Rods, Rod Bipolar Cells, and Ganglion Cells
A family of light responses is shown for (A) a *Rv*^{+/+} rod for flashes delivering 6.2, 12, 25, 49, 94, and 190 photons/ μm^2 (all in effective 501 nm photons); (B) a *Rv*^{+/+} rod bipolar cell for flashes delivering 0.62, 1.2, 2.5, 5.0, 9.9, 20, and 40 photons/ μm^2 ; (C) a *Rv*^{+/+} ON α ganglion cell for flashes delivering 0.025, 0.051, 0.10, 0.20, 0.41, 0.81, and 1.6 photons/ μm^2 ; (D) a *Rv*^{-/-} rod for flashes delivering 5.5, 11, 22, 43, 87, 170, and 350 photons/ μm^2 ; (E) a *Rv*^{-/-} rod bipolar cell for flashes delivering 0.58, 1.2, 2.3, 4.7, 9.3, 19, 37, and 75 photons/ μm^2 ; and (F) a *Rv*^{-/-} ganglion cell for flashes delivering 0.012, 0.025, 0.051, 0.10, 0.20, 0.41, 0.81, and 1.6 photons/ μm^2 . The arrow in (E) and (F) indicates a secondary peak prominent in *Rv*^{-/-} rod bipolar and ganglion cell responses. (G) Stimulus-response curve for the rods in (A) and (D). The data have been fit with an exponential saturation function (see [Experimental Procedures](#)), with $k = 0.032$ (or $I_{1/2} = 22$ photons/ μm^2). (H) Stimulus-response curve for the rod bipolar cells in (B) and (E). The data have been fit with a Hill equation (see [Experimental](#)

[Procedures](#)). For *Rv*^{+/+} rod bipolar cells, $n = 1.60$ and $I_{1/2} = 6.4$ photons/ μm^2 , and for *Rv*^{-/-} rod bipolar cells, $n = 1.51$ and $I_{1/2} = 5.8$ photons/ μm^2 . Flashes were all 10 ms and delivered at time = 0. Bandwidth is 30 Hz for rods and 50 Hz for rod bipolar and ganglion cells.

In particular, at the lowest light levels probed the responses of *Rv*^{+/+} and *Rv*^{-/-} rod bipolar cells showed a similar supralinear dependence on flash strength ([Table 1](#)); this supralinear dependence is produced by post-synaptic saturation ([Sampath and Rieke, 2004](#)).

The kinetics of rod bipolar responses from *Rv*^{+/+} and *Rv*^{-/-} retinas differed. A secondary oscillation in the rod bipolar responses (cf. [Field and Rieke, 2002a](#)) was more pronounced in *Rv*^{-/-} cells ([Figure 2E](#), arrow). In addition, *Rv*^{-/-} rod bipolar responses had a shorter time to peak and integration time ([Table 1](#)). As described below, the differences in kinetics of the rod bipolar responses were not inherited from the rod outer segment responses.

ON α Ganglion Cells

We compared flash responses from ON α ganglion cells in *Rv*^{+/+} and *Rv*^{-/-} retinas to determine how Rv affected the retinal output. [Figures 2C](#) and [2F](#) compare families of light-evoked synaptic currents (see [Experimental Procedures](#)) from ganglion cells in whole-mount *Rv*^{+/+} and *Rv*^{-/-} retinas. Responses of *Rv*^{-/-} ganglion cells, like those of rod bipolar cells, returned abruptly to

baseline. Secondary oscillations appeared in response to the brightest flashes in *Rv*^{-/-} ganglion cells at a similar time to the secondary oscillation in rod bipolar cell responses ([Figures 2E](#) and [2F](#), arrows). Like the rod and rod bipolar responses, the time to peak and integration time of the dim flash responses of *Rv*^{-/-} ganglion cells were shorter than those of *Rv*^{+/+} ganglion cells ([Table 1](#)).

Shortening of Rod Photoresponses Does Not Account for the Shortening of Rod Bipolar and Ganglion Cell Responses

The absence of Rv abbreviated responses of rods, rod bipolar cells, and ganglion cells. To determine whether the alterations in rod responses could account for the effects on downstream cells, we compared the time courses of flash responses from each cell type. [Figure 3A](#) compares averaged responses of *Rv*^{+/+} and *Rv*^{-/-} rods to dim flashes. Linear range responses that suppressed between 0% and 25% of the maximum photocurrent were pooled to evaluate the response per photoisomerization ([Baylor et al., 1979a](#)). A single photoisomerization suppressed $\sim 5\%$ of the circulating

Table 1. Characterization of the Sensitivity and Time Course of the Responses of Retinal Neurons^a

| | Rods | | Rod Bipolar Cells | | ON α Ganglion Cells | |
|---------------------------------------|--------------------------|--------------------------|--------------------------|--------------------------|----------------------------|--------------------------|
| | <i>Rv</i> ^{+/+} | <i>Rv</i> ^{-/-} | <i>Rv</i> ^{+/+} | <i>Rv</i> ^{-/-} | <i>Rv</i> ^{+/+} | <i>Rv</i> ^{-/-} |
| $I_{1/2}$ ^b | 19 \pm 1 (22) | 20 \pm 2.5 (14) | 7.0 \pm 0.6 (27) | 6.2 \pm 0.6 (32) | 0.36 \pm 0.10 (19) | 0.31 \pm 0.08 (21) |
| n | | | 1.60 \pm 0.06 (27) | 1.70 \pm 0.06 (32) | 1.37 \pm 0.11 (19) | 1.41 \pm 0.12 (21) |
| τ_{int} ^c (ms) | 328 \pm 22 (12.8) | 253 \pm 21 (4.8) | 115 \pm 7.1 (10.7) | 91 \pm 9.7 (14.6) | 120 \pm 16 (4.8) | 73 \pm 6.1 (2.6) |
| T_{peak} ^c (ms) | 204 \pm 12 (12.8) | 229 \pm 13 (4.8) | 154 \pm 5.0 (10.7) | 131 \pm 7.6 (14.6) | 141 \pm 8.6 (4.8) | 125 \pm 4.5 (2.6) |

^aAll values given as the mean \pm SEM (number of cells).

^b $I_{1/2}$ is the half-maximal flash strength, in units of 501 nm photons/ μm^2

^cValues for numbers of cells are weighted based on the number of trials per cell. An "effective" number of cells was determined by dividing the total trials across all cells by the number of trials for the cell where the greatest number was recorded. The effective number essentially normalizes the contribution of each cell to the cell with the most trials, providing a more accurate estimate of the SEM.

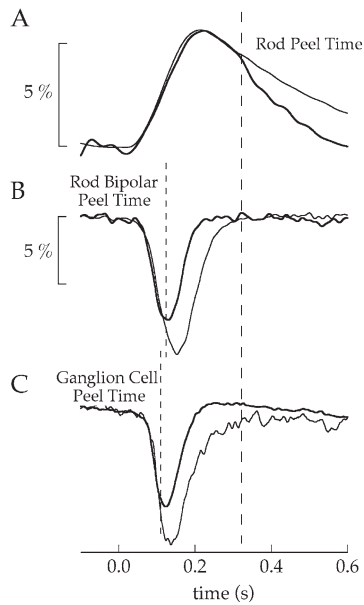


Figure 3. Recoverin Effects in the OS Do Not Explain Changes in Rod Bipolar or Ganglion Cell Responses

(A) Responses of $Rv^{+/+}$ (light) and $Rv^{-/-}$ (dark) rods to single photons. Single photon responses were calculated by dividing dim flash responses (<25% R_{max}) by the average number of photoisomerizations delivered (assuming a collecting area of $0.5 \mu\text{m}^2$; Field and Rieke, 2002b). Single photon responses were determined from 3763 responses across 22 $Rv^{+/+}$ rods, and 3269 responses across 14 $Rv^{-/-}$ rods. The scale bar shows a 5% suppression of the circulating current. The time at which the $Rv^{+/+}$ and $Rv^{-/-}$ rod responses peel from each other is marked by a dashed line ~ 310 ms after the flash.

(B) The response of rod bipolar cells for 1 Φ per rod was determined in a similar manner as for the rods in (A) for responses that ranged between 5% and 25% of R_{max} . Please note that the relationship between response amplitude and flash strength in mouse rod bipolar cells is nonlinear (Sampath and Rieke, 2004). The $Rv^{+/+}$ response was the average of 639 responses across 27 rod bipolar cells resulting from an average flash strength of $1.8 \text{ photons}/\mu\text{m}^2$. The $Rv^{-/-}$ response was the average of 261 responses across 32 rod bipolar cells resulting from an average flash strength of $1.9 \text{ photons}/\mu\text{m}^2$. Included in all data shown are cells from the same animals used for behavior experiments. The rod bipolar peel time is marked by a dashed line ~ 115 ms after the flash, much earlier than the peel away time of the rod responses in (A).

(C) The average response of ON α ganglion cells that ranged between 5% and 10% of R_{max} was determined for $Rv^{+/+}$ and $Rv^{-/-}$ mice. The $Rv^{+/+}$ response was the average of 121 responses across 21 ganglion cells, and the $Rv^{-/-}$ response was the average of 207 responses across 17 ganglion cells. Variability in the sensitivity of ganglion cell responses (see Table 1) prevented scaling the responses by flash strength. Instead, response kinetics were compared by matching rising phases of the responses. This strategy delays the peel away time to the latest possible point. The maximal possible peel away time is marked by a dashed line ~ 110 ms after the flash.

current in both $Rv^{+/+}$ and $Rv^{-/-}$ rods. Although responses of $Rv^{+/+}$ and $Rv^{-/-}$ rods initially followed the same trajectory, they diverged 310 ms after the flash, and the $Rv^{-/-}$ response recovered more quickly (Figure 3A, dashed line).

If altered rod responses caused altered rod bipolar responses, we would expect, by causality, the first

~ 300 ms of $Rv^{+/+}$ and $Rv^{-/-}$ bipolar responses to be identical. This was not the case. Figure 3B compares rod bipolar cell responses from $Rv^{+/+}$ and $Rv^{-/-}$ retinas. Just as for rods, we calculated the average response per photoisomerization using only responses to the dimmest flashes (5%–25% R_{max}). Responses in this range had similar kinetics. Surprisingly, the $Rv^{+/+}$ and $Rv^{-/-}$ responses diverged ~ 115 ms after the flash (Figure 3B), much earlier than the divergence of the rod responses. In addition, the rod bipolar response was nearly complete by the time $Rv^{+/+}$ and $Rv^{-/-}$ rod responses began to diverge. Thus, the late divergence in rod responses cannot account for the early divergence of rod bipolar responses. Together, these observations indicate that Rv in rods acts at a site distinct from its action in the outer segment. It is this action of Rv that dominates the effect of Rv on the time course of the rod bipolar response.

The responses of ganglion cells resembled the rod bipolar cell responses. Figure 3C plots averaged responses for the smallest ganglion cell responses (5%–10% R_{max}). The time course of the dimmest responses sped up with increasing size, precluding averaging of responses over a larger amplitude range as for the rod bipolar cells. In addition, variability in the sensitivity of these cells (see Table 1) prevented a scaling of the responses per photon. Thus, to compare the time courses we scaled the averaged responses of $Rv^{-/-}$ responses to delay the time at which they separated from $Rv^{+/+}$ responses as much as possible. $Rv^{-/-}$ ganglion cell responses diverged from the $Rv^{+/+}$ responses ~ 110 ms after the flash, similar to the time at which rod bipolar responses diverged. Thus, the altered time course of the rod bipolar responses can largely or entirely account for that of the ganglion cells. However, as for the rod bipolar responses, the altered ganglion cell responses could not be explained by changes in the rod outer segment responses.

Recoverin Is Present throughout the Entire Rod Cell
Our findings indicate that Rv influences signal transfer between rods and rod bipolar cells. This implies that it must be present in rod compartments other than the OS. We evaluated the subcellular distribution of Rv in dark-adapted mouse retinas by immunocytochemical labeling (Figure 4A). Although some Rv was in the OS, most was present in the inner segment and synaptic terminal. This distribution was confirmed by serial tangential sectioning of the retina, electrophoretic separation of denatured proteins, and quantitative immunoblotting (Sokolov et al., 2002; Sokolov et al., 2004). This method is less susceptible to artifacts like epitope masking, but it has lower sensitivity. Figure 4B shows that Rv was present throughout the entire rod cell, but a majority was in the cell bodies. In dark-adapted retinas, only 11% of Rv was in the OS.

Discussion

Recoverin is highly conserved and expressed in all vertebrate retinas, suggesting that it is important for vision. Indeed, visual sensitivity is compromised in $Rv^{-/-}$ mice (Figure 1). The inactivation of the Rv gene in mice

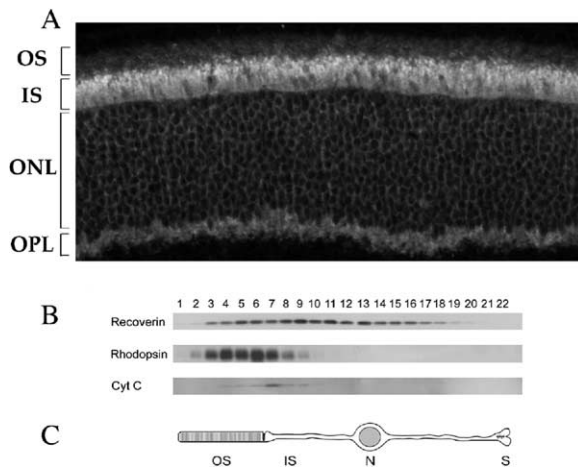


Figure 4. Distribution of Rv in the Mouse Retina

(A) Rv was localized by immunofluorescence of sections of dark-adapted retinas. Staining of Rv at the synapse is easily visualized, most likely because it is concentrated into a small volume within the synaptic terminal.

(B) Rv was also localized quantitatively by immunoblotting homogenates of serial sections. Rv immunoreactivity is shown versus longitudinal position of the section along the rod. Peaks of rhodopsin (an OS marker) and cytochrome oxidase (an inner segment mitochondrial marker) are indicated by arrows.

(C) The cartoon illustrates a schematic drawing of the rod cell where the respective cellular compartments are aligned with the corresponding lanes of the immunoblot. The nucleus location shown is arbitrary. In the retina, rod nuclei are stacked within the outer nuclear layer. Staining of Rv in the synaptic terminal fractions was variable in these types of experiments. It may be significantly diluted because of the small volume of the rod synaptic terminal relative to the section thickness.

is functionally selective and does not lead to measurable compensatory changes of any mRNAs or the levels of known phototransduction proteins other than Rv (Makino et al., 2004).

Recoverin and Signal Transfer between Rods and Rod Bipolar Cells

The central finding of our study is that Rv enhances signal transfer between rods and rod bipolar cells and that this enhancement can account for its impact on visual sensitivity. An effect of Rv on signal transmission must derive from an action downstream of the OS, and indeed Rv is present throughout the rod (Figure 4). Its influence could be direct or indirect. Rv could influence Ca^{2+} buffering, inner segment conductances, or the synaptic release of glutamate. Rv is a member of the neuronal calcium sensor (NCS) protein family, and other NCS proteins have been shown to influence synaptic facilitation (see Burgoyne and Weiss, 2001) and gene expression (reviewed by Ikura et al., 2002). Regardless of the mechanism, Rv prolongs the pause in glutamate release during the rod single photon response (Figure 3B). Several possible mechanisms are discussed in more detail below.

Ca^{2+} Buffering

Rv- Ca^{2+} contributes ~15% of exchangeable Ca^{2+} in the OS (Makino et al., 2004). A similar contribution to Ca^{2+}

buffering at the synaptic terminal could influence glutamate release. Ca^{2+} buffering would not influence the equilibrium concentration of free Ca^{2+} , so dark glutamate release should not be influenced by Rv. However, free Ca^{2+} would change more rapidly in $Rv^{-/-}$ rods. This is consistent with faster recovery of bipolar responses in $Rv^{-/-}$ retinas (Figure 3B). A steeper rising phase might also be expected, but the initial clearance of cytoplasmic Ca^{2+} from the rod terminal could be limited by another mechanism, or the clearance of glutamate from the synaptic cleft may not instantaneously follow changes in glutamate release.

Regulation of Inner Segment Conductances

An effect of Rv on inner segment conductances could shape the rod's voltage response and prolong the hyperpolarization during a response to a photon. This would require that Rv modulate an inner segment conductance that normally helps produce a close temporal correspondence between the OS current response and inner segment voltage change (Baylor and Nunn, 1986). Without Rv, this conductance could speed the voltage change relative to the current change.

Interactions with Synaptic Machinery

The NCS protein Frequentin (also called NCS-1) enhances synaptic facilitation either by direct interaction with release machinery (Pongs et al., 1993; Sippy et al., 2003) or by facilitation of the synaptic Ca^{2+} current (Tsujiimoto et al., 2002). Rods depolarize in darkness and hyperpolarize with light absorption, so the changes in synaptic Ca^{2+} are opposite to most conventional neurons. The influence of Rv on synaptic transmission would therefore need to be opposite to that of NCS-1; i.e., Ca^{2+} -free Rv would delay recovery of glutamate release to the dark level. A mechanism of this type could explain why the dark rate of glutamate release appears similar in $Rv^{+/+}$ and $Rv^{-/-}$ rods and why fast changes in synaptic Ca^{2+} could prolong rod bipolar responses in $Rv^{+/+}$ mice (Figure 3B).

Recoverin's Influence on Vision

Vision in dim light is mediated by the rod bipolar pathway in mammals (Deans et al., 2002; reviewed by Field et al., 2005). Rods are the only cells in this pathway that express Rv. The absence of Rv in rods reduces visual sensitivity ~4 fold. The rod-mediated responses in $Rv^{+/+}$ and $Rv^{-/-}$ retinas show smaller changes, e.g., the integration times of rod, rod bipolar, and ganglion cell responses are reduced 30%–40%. At the level of ganglion cells, the difference in integration time of light-evoked synaptic currents cannot explain the ~4 fold change in visual sensitivity. Therefore, the differences must be amplified during later stages of visual processing. For example, a nonlinear relationship between synaptic currents in ganglion cells and spike generation could contribute to larger differences in behavior (Galaretta and Hestrin, 2001; Pouille and Scanziani, 2001).

What Segments of the Rod Photoresponse Are Important for Processing at Visual Threshold?

The comparison shown in Figure 3 identifies which segments of the rod response are most important for visual processing. Rod bipolar and ganglion cell responses are nearly complete by the time rod responses peak. A

similar but less direct comparison has been made by electroretinography (Robson and Frishman, 1995). Thus, the falling phase of rod responses cannot contribute to processing of rod signals near visual threshold. The waveform of the single photon responses is highly reproducible (Baylor et al., 1979b; Rieke and Baylor, 1998; Whitlock and Lamb, 1999; Field and Rieke, 2002b), but the greatest variation occurs after the response has reached its peak (Rieke and Baylor, 1998; Field and Rieke, 2002b). Taken altogether, these results suggest that only the rising phase of the response provides information about single photon absorption to downstream neurons. Consistent with this interpretation, humans with a null mutation in rhodopsin kinase, and presumably prolonged rod photoreponses (Chen et al., 1999), have normal rod thresholds when fully dark adapted (Cideciyan et al., 1998).

Experimental Procedures

Mice

Inactivation of the *Rv* gene was described in a previous report (Makino et al., 2004). *Rv*^{-/-} mice were inbred for several generations in a mixed 129SvEv/C57Bl6 background and then outcrossed with C57Bl6 to produce heterozygotes. The heterozygotes were then inbred to produce litters of *Rv*^{+/+}, *Rv*^{+/-}, and *Rv*^{-/-} mice. For most of the experiments in this report, we used siblings from these crosses. Additional studies were also done using inbred *Rv*^{-/-} mice with *Rv*^{+/+} control mice produced by inbreeding nontransgenic 129SvEv × C57Bl6 parents. Analyses of both sets of mice demonstrated the same effects of *Rv* independently of genetic background in every type of experiment described. Mice were 2–4 months old and maintained on a 12/12 hr light-dark cycle.

Water Maze and Pupil Measurement

A vision-dependent behavior, the ability to find a black wall in a white water maze, was used to establish visual threshold (see also Hayes and Balkema, 1993). Each mouse received four training trials per day for at least 10 days under ambient light. Times to find the platform ranged from 1 to 45 s. In darkness or in dim light, a mouse that did not find the ramp within 45 s was guided to it. The black wall and platform were rinsed and moved randomly between trials. Testing was performed under controlled illumination, beginning with the brightest illumination and decreasing one log unit in intensity per day using neutral density filters until there was a significant increase in the time to find the platform. Mice were then tested at that level for several days to establish the most efficient search strategy. When the time to swim to the platform was constant, illumination was lowered further. The process was repeated until the average time to find the platform was the same as in complete darkness (~20 s).

We determined photon flux by measuring the energy and spectral composition of light from the halogen lamps reflected from the white walls of the maze. Using the absorbance spectrum of rhodopsin, we calculated photon flux in units of equivalent photons at peak spectral sensitivity (~501 nm). To estimate the number of absorbed photons per second at visual threshold, we converted the photon flux at the cornea to an equivalent Rh^* , using Equation 1 of Lyubarsky and Pugh (1996). We evaluated pupil areas of mice in the maze using an IR-sensitive video camera with macro lens (model DCR-TRV22, Sony Corporation) using methods similar to those previously published (Pennesi et al., 1998). Unanesthetized mice were restrained gently by hand at the center of the water maze and exposed to background lights delivered from the same lamp and in the same configuration as during the behavioral task. The eye was illuminated with infrared diodes (RadioShack), and short video clips (5–10 s) were collected once the mouse adapted for 1 min to the background illumination. Pupil areas were determined from single frames of these videos. The light intensity at each background was scaled based on changes in pupil area.

Recording Light-Evoked Currents from Rods, Rod Bipolar Cells, and Ganglion Cells

In all recordings, cells were superfused at 35°C–37°C with bicarbonate-buffered Ames medium (Sigma). Rod photocurrents were measured by drawing rod outer segments into suction electrodes (Baylor et al., 1979a). Rod bipolar cell responses were measured with whole-cell voltage-clamp recordings ($V_m = -60$ mV) from cells in retinal slices prepared as described previously (Armstrong-Gold and Rieke, 2003). The internal solution for these experiments was as follows: 125 mM K-Aspartate, 10 mM KCl, 10 mM HEPES, 5 mM NMG-HEDTA, 0.5 mM CaCl₂, 1 mM ATP-Mg, 0.2 mM GTP-Mg. pH was adjusted to 7.2 with NMG-OH. ON α ganglion cell light responses were also measured under voltage clamp ($V_m = -60$ mV) from a whole-mount retina. Cells were selected based on the following criteria: large cell bodies and inward currents at the onset of light but not at the onset of darkness (Peng et al., 2003). The internal solution for ganglion cell recordings was as follows: 90 mM Cs-Methanesulfonate, 20 mM TEA-Cl, 20 mM HEPES, 10 mM EGTA, 5 mM ATP-Mg, 0.5 mM GTP-Mg, 2 mM QX-314; pH was adjusted to 7.3 with CsOH. This solution prevented ganglion cells from spiking so synaptic currents could be isolated. All light-evoked currents were digitized at 1 kHz after low-pass filtering at 30 Hz for rods, and 300 Hz for rod bipolar and ganglion cells.

The sensitivity and kinetics of light-evoked currents in rods, rod bipolar cells, and ganglion cells were measured in response to 10 ms or 30 ms flashes from an LED ($\lambda_{max} = 470$ nm), whose strength varied from those generating a just-measurable response to flashes that generate a maximal response. For rod photoreceptors, the response amplitude normalized to the brightest flash was plotted versus flash strength and fit with an exponential saturation equation:

$$\frac{R}{R_{max}} = 1 - e^{-kt}$$

where R/R_{max} is the normalized response amplitude, ϕ is the flash strength with a half-maximal flash strength ($I_{1/2}$) of $\log(2)/k$. For rod bipolar and ganglion cells, the fraction of the maximal amplitude for each flash was plotted versus the flash strength and was least-squares fit with a Hill Equation:

$$\frac{R}{R_{max}} = \frac{1}{1 + (I_{1/2}/I)^n}$$

where $I_{1/2}$ is the flash strength generating a half-maximal response, and n is Hill exponent relating the flash strength to the response amplitude.

Immunofluorescence

Immunocytochemical analyses were performed as described (McGinnis et al., 1997). Balb/cJ mice were dark adapted >12 hr. *Rv* was localized using a rabbit antibody against the last 28 amino acids of mouse *Rv*. The signal was amplified with biotinylated horse anti-rabbit IgG followed by streptavidin conjugated to Alexa Green 350 (Molecular Probes) (McGinnis et al., 1997). Sections were examined using a Nikon Eclipse 800 microscope with 20× objective (0.75 NA), and images were captured digitally. The image shown is representative of three sections from three mice.

Serial Sectioning and Immunoblotting

The method was as described (Sokolov et al., 2002) with additional optimization (Sokolov et al., 2004). Wild-type mice were dark adapted overnight and euthanized. Retinas were mounted flat, and sequential tangential sections were isolated and analyzed by immunoblotting with the following antibodies: p26 anti-*Rv* rabbit polyclonal (a gift from A.M. Dizhoor), anti-cytochrome oxidase subunit IV (A-6431 from Molecular Probes), and monoclonal anti-rhodopsin 4D2 (a gift from R.S. Molday). Protein bands were visualized using an ECL Detection System (Amersham). To average data among individual experiments, data sets were aligned with the rhodopsin peak set at the same position (section 4).

Supplemental Data

The Supplemental Data include Supplemental Experimental Procedures and one supplemental figure and can be found with this article online at <http://www.neuron.org/cgi/content/full/46/3/413/DC1/>.

Acknowledgments

This work was supported by NEI grants EY06641 (J.B.H.), NRSA EY14784 (A.P.S.), EY10336 (V.Y.A.), EY13050 (J.F.M.), EY12703 (J.C.), and EY11850 (F.R.) and core grant EY12190 (J.F.M.). V.Y.A. is supported by the Massachusetts Lions Eye Research Fund, and J.C. and J.F.M. are supported by Research to Prevent Blindness. We are particularly grateful to the late Grant Balkema, who gave us expert assistance in setting up the water maze behavior experiments, and John Robson for helpful discussions. We thank Irina Ankoudinova for assistance with training mice; Thuy Doan for help with suction electrode recordings; Felice Dunn for help with whole-mount recordings; Lynn Trieu for help with serial sectioning analysis; and Janice Lem for providing rod transducin knockout mice.

Received: September 28, 2004

Revised: December 10, 2004

Accepted: April 7, 2005

Published: May 4, 2005

References

Armstrong-Gold, C.E., and Rieke, F. (2003). Bandpass filtering at the rod to second-order cell synapse in salamander (*Ambystoma tigrinum*) retina. *J. Neurosci.* **23**, 3796–3806.

Barlow, H.B., Levick, W.R., and Yoon, M. (1971). Responses to single quanta of light in retinal ganglion cells of the cat. *Vision Res.* **23**, 87–101.

Baylor, D.A., and Nunn, B.J. (1986). Electrical properties of the light-sensitive conductance of rods of the salamander *Ambystoma tigrinum*. *J. Physiol.* **371**, 115–145.

Baylor, D.A., Lamb, T.D., and Yau, K.-W. (1979a). The membrane current of single rod outer segments. *J. Physiol.* **288**, 589–611.

Baylor, D.A., Lamb, T.D., and Yau, K.-W. (1979b). Responses of retinal rods to single photons. *J. Physiol.* **288**, 613–634.

Baylor, D.A., Nunn, B.J., and Schnapf, J.L. (1984). The photo-current, noise and spectral sensitivity of rods of the monkey *Macaca fascicularis*. *J. Physiol.* **357**, 575–607.

Burgoyne, R.D., and Weiss, J.L. (2001). The neuronal calcium sensor family of Ca²⁺-binding proteins. *Biochem. J.* **353**, 1–12.

Calvert, P.D., Krasnoperova, N.V., Lyubarsky, A.L., Isayama, T., Nicolo, M., Kosaras, B., Wong, G., Gannon, K.S., Margolskee, R.F., Sidman, R.L., et al. (2000). Phototransduction in transgenic mice after the targeted deletion of the rod transducin alpha-subunit. *Proc. Natl. Acad. Sci. USA* **97**, 13913–13918.

Chen, J., Makino, C.L., Peachey, N.S., Baylor, D.A., and Simon, M.I. (1995). Mechanisms of rhodopsin inactivation in vivo as revealed by a COOH-terminal truncation mutant. *Science* **267**, 374–377.

Chen, C.-K., Burns, M.E., Spencer, M., Niemi, G.A., Chen, J., Hurley, J.B., Baylor, D.A., and Simon, M.I. (1999). Abnormal photoreponses and light-induced apoptosis in rods lacking rhodopsin kinase. *Proc. Natl. Acad. Sci. USA* **96**, 3718–3722.

Cideciyan, A.V., Zhao, X., Nielsen, L., Khani, S.C., Jacobson, S.G., and Palczewski, K. (1998). Null mutation in the rhodopsin kinase gene slows recovery kinetics of rod and cone phototransduction in man. *Proc. Natl. Acad. Sci. USA* **95**, 328–333.

Dacheux, R.F., and Raviola, E. (1986). The rod pathway in the rabbit retina: a depolarizing bipolar and amacrine cell. *J. Neurosci.* **6**, 331–345.

Deans, M.R., Volgyi, B., Goodenough, D.A., Bloomfield, S.A., and Paul, D.A. (2002). Connexin36 is essential for transmission of rod-mediated visual signals in the mammalian retina. *Neuron* **36**, 703–712.

Erickson, M.A., Lagnado, L., Zozulya, S., Neubert, T.A., Stryer, L., and Baylor, D.A. (1998). The effect of recombinant recoverin on the photoresponse of truncated rod photoreceptors. *Proc. Natl. Acad. Sci. USA* **95**, 6474–6479.

Field, G.D., and Rieke, F. (2002a). Nonlinear signal transfer from mouse rods to bipolar cells and implications for visual sensitivity. *Neuron* **34**, 773–785.

Field, G.D., and Rieke, F. (2002b). Mechanisms regulating variability of the single photon responses of mammalian rod photoreceptors. *Neuron* **35**, 733–747.

Field, G.D., Sampath, A.P., and Rieke, F. (2005). Retinal processing near absolute threshold: from behavior to mechanism. *Annu. Rev. Physiol.* **67**, 491–514.

Galaretta, M., and Hestrin, S. (2001). Spike transmission and synchrony detection in networks of GABAergic interneurons. *Science* **292**, 2295–2299.

Gray-Keller, M.P., Polans, A.S., Palczewski, K., and Detwiler, P.B. (1993). The effect of recoverin-like calcium-binding proteins on the photoresponse of retinal rods. *Neuron* **10**, 523–531.

Hayes, J.M., and Balkema, G.W. (1993). Elevated dark-adapted thresholds in hypopigmented mice measured with a water maze screening apparatus. *Behav. Genet.* **23**, 395–403.

Ikura, M., Osawa, M., and Ames, J.B. (2002). The role of calcium-binding proteins in the control of transcription: structure to function. *Bioessays* **24**, 625–636.

Kawamura, S. (1993). Rhodopsin phosphorylation as a mechanism of cyclic GMP phosphodiesterase regulation by S-modulin. *Nature* **362**, 855–857.

Lyubarsky, A.L., and Pugh, E.N., Jr. (1996). Recovery phase of the murine rod photoresponse reconstructed from electroretinographic recordings. *J. Neurosci.* **16**, 563–571.

Makino, C.L., Dodd, R.L., Chen, J., Burns, M.E., Roca, A., Simon, M.I., and Baylor, D.A. (2004). Recoverin regulates light-dependent phosphodiesterase activity in retinal rods. *J. Gen. Physiol.* **123**, 729–741.

McGinnis, J.F., Strepanik, P.L., Jeriangprasert, S., and Lerious, V. (1997). Functional significance of recoverin localization in multiple retina cell types. *J. Neurosci. Res.* **50**, 487–495.

Milam, A.H., Dacey, D.M., and Dizhoor, A.M. (1993). Recoverin immunoreactivity in mammalian cone bipolar cells. *Vis. Neurosci.* **10**, 1–12.

Peng, J.-J., Gao, F., and Wu, S.M. (2003). Light-evoked excitatory and inhibitory synaptic inputs to ON and OFF α ganglion cells in the mouse retina. *J. Neurosci.* **23**, 6063–6073.

Pennesi, M.E., Lyubarsky, A.L., and Pugh, E.N., Jr. (1998). Extreme responsiveness of the pupil of the dark-adapted mouse to steady retinal illumination. *Invest. Ophthalmol. Vis. Sci.* **39**, 2148–2156.

Pongs, O., Lindermeier, J., Zhu, X.R., Theil, T., Engelkamp, D., Kraht-Jentgens, I., Lambrecht, H.-G., Koch, K.W., Schwemer, J., Rivo-secchi, R., et al. (1993). Frequenin—a novel calcium-binding protein that modulates synaptic efficacy in the *Drosophila* nervous system. *Neuron* **11**, 15–28.

Pouille, F., and Scanziani, M. (2001). Enforcement of temporal fidelity in pyramidal cells by somatic feed-forward inhibition. *Science* **293**, 1159–1163.

Rieke, F., and Baylor, D.A. (1998). The origin of reproducibility in the responses of retinal rods to single photons. *Biophys. J.* **75**, 1836–1857.

Robson, J.G., and Frishman, L.J. (1995). Response linearity and kinetics of the cat retina: the bipolar cell component of the dark-adapted electroretinogram. *Vis. Neurosci.* **12**, 837–850.

Sampath, A.P., and Rieke, F. (2004). Selective transmission of single photon responses by saturation at the rod-to-rod bipolar synapse. *Neuron* **41**, 431–443.

Sippy, T., Cruz-Martín, A., Jeromin, A., and Schweizer, F.E. (2003). Acute changes in short-term plasticity at synapses with elevated levels of neuronal calcium sensor-1. *Nat. Neurosci.* **6**, 1031–1038.

Sokolov, M., Lyubarsky, A.L., Strissel, K.J., Savchenko, A.B., Govardovskii, V.I., Pugh, E.N., Jr., and Arshavsky, V.Y. (2002). Massive

light-driven translocation of transducin between the two major compartments of rod cells: a novel mechanism of light adaptation. *Neuron* 34, 95–106.

Sokolov, M., Strissel, K.J., Leskov, I.B., Michaud, N.A., Govardovskii, V.I., and Arshavsky, V.Y. (2004). Phosducin facilitates light-driven transducin translocation in rod photoreceptors: Evidence from the phosducin knockout mouse. *J. Biol. Chem.* 279, 19149–19156.

Sterling, P., Freed, M.A., and Smith, R.G. (1988). Architecture of rod and cone circuits to the On-beta ganglion cell. *J. Neurosci.* 8, 623–642.

Tsujimoto, T., Jeromin, A., Saitoh, N., Roder, J.C., and Takahashi, T. (2002). Neuronal calcium sensor 1 and activity-dependent facilitation of P/Q-type calcium currents at presynaptic nerve terminals. *Science* 295, 2276–2279.

Walraven, J., Enroth-Cugell, C., Hood, D.C., MacLeod, D.I.A., and Schnapf, J.L. (1990). The control of visual sensitivity: Receptor and postreceptor processes. In *The Neurophysiological Foundations of Visual Perception*, L. Spillman and J. Werner, eds. (San Diego, CA: Academic Press), pp. 53–101.

Whitlock, G.G., and Lamb, T.D. (1999). Variability in the time course of single photon responses from toad rods: termination of rhodopsin's activity. *Neuron* 23, 337–351.